Cross sections for low-energy inelastic Mg + H and $Mg^+ + H^-$ collisions

A. K. Belyaev,[1,2] P. S. Barklem,[2] A. Spielfiedel,[3] M. Guitou,[4] N. Feautrier,[3] D. S. Rodionov,[1] and D. V. Vlasov[1]

[1]*Department of Theoretical Physics, Herzen University, St. Petersburg 191186, Russia*

[2]*Department of Physics and Astronomy, Uppsala University, Box 516, S-75120 Uppsala, Sweden*

[3]*LERMA, Observatoire de Paris, 92195 Meudon Cedex, France*

[4]*Université Paris-Est, Laboratoire Modélisation et Simulation Multi-Echelle, UMR 8208 CNRS, 5 Boulevard Descartes, 77454 Marne-la-Vallée, France*

(Received 3 November 2011; published 2 March 2012)

We report full quantum scattering calculations for low-energy near-threshold inelastic cross sections in Mg + H and $Mg^+ + H^-$ collisions. The calculations include all transitions between the eight lowest adiabatic MgH($^2\Sigma^+$) molecular states, with the uppermost of those diabatically extended to the ionic molecular state in the asymptotic region. This allows us to treat the excitation processes between the seven lowest atomic states of magnesium in collisions with hydrogen atoms, as well as the ion-pair production and the mutual neutralization processes. The collision energy range is from threshold up to 10 eV. These results are important for astrophysical modeling of spectra in stellar atmospheres. The processes in question are carefully examined and several process mechanisms are found. Some mechanisms are determined by interactions between ionic and covalent configurations at relatively large internuclear distances, while others are based on short-range nonadiabatic regions due to interactions between covalent configurations.

DOI: 10.1103/PhysRevA.85.032704 PACS number(s): 34.50.Fa

I. INTRODUCTION

Data on low-energy inelastic collision processes on atoms are needed in many fields of physics, in particular, for nonequilibrium modeling of spectral line formation in stellar atmospheres, and thus in measurement of chemical composition and other stellar properties of astrophysical interest [1]. The need for data for inelastic collisions due to hydrogen atom impact at low energies on magnesium, an element of significant astrophysical importance (e.g., [2]), has been motivated in earlier work [3] where some of the present authors calculated such data for transitions between the three lowest-lying atomic states.

It was shown in Ref. [3] that the transitions between the lowest-lying MgH($^2\Sigma^+$) molecular states dominate over transitions involving states of other symmetries, in particular, the $^2\Pi$ state. In the standard adiabatic Born-Oppenheimer approach, states of the same symmetry are coupled via nonadiabatic radial couplings. The ionic configuration, $Mg^+ + H^-$, has $^2\Sigma^+$ symmetry, and thus there exists interactions between ionic and covalent configurations in this symmetry, leading to avoided ionic crossings amongst these molecular states in the adiabatic representation. These interactions lead to substantial radial coupling between molecular states of this symmetry at significant internuclear distances and thus represent the most important mechanism for nonadiabatic transitions among low-lying states. This mechanism has also been seen to be important in Li + H [4,5] and Na + H collisions [6–8]. Application to astrophysical models in the cases of Li and Na has shown the importance of ion-pair production and mutual neutralization processes [$X(nl) + H \rightleftharpoons X^+ + H^-$, where X is the atom of interest], which arise naturally due to the influence of the ionic configuration.

In this work, we extend the earlier work in Ref. [3] through a calculation including eight $^2\Sigma^+$ states up to and including the ionic channel, and thus covering the ion-pair production and mutual neutralization processes in addition to excitation processes. This results in a data set of sufficient scope for astrophysical models. The second goal of this paper is to study mechanisms of different inelastic processes in low-energy Mg + H and $Mg^+ + H^-$ collisions.

II. QUANTUM-CHEMICAL DATA

A. *Ab initio* calculations

Although our present interest is focused on dynamics involving the first eight $^2\Sigma^+$ molecular states, all electronic states (with $^{2,4}\Sigma^+$, $^{2,4}\Pi$, and $^2\Delta$ symmetries) arising from Mg + H(^2S_g) for energies up to about 6 eV above the lowest atomic asymptote Mg($3s^2\,^1S$) + H(^2S_g) were calculated, as well as the nonadiabatic couplings between these states. The calculations use the strategy described in detail in Ref. [9]. Results using different basis sets and active spaces were compared and it was concluded that the aug-cc-pCVQZ $(20s,16p,7d,5f,3g) \rightarrow [10s,9p,7d,5f,3g]$ scheme of Woon and Dunning Jr. [10] for Mg and aug-cc-pV5Z [11] for the H atom and an active space including 10σ, 5π, and 1δ orbitals gave very good results. The $1s$, $2s$, and $2p$ orbitals of Mg were kept closed in the calculations. Such large active space and basis sets are essential to correctly represent the eight lowest $^2\Sigma^+$ states as avoided crossings occur due to the Mg^+-H^- ionic configuration [9]. The accuracy necessary for the description of the mixing of the electronic states was achieved first by making state-averaged complete active space self-consistent-field (CASSCF) [12] calculations with the active space of 17 orbitals mentioned above. Then the CASSCF wave functions were taken as a reference for internally contracted multireference configuration interaction (MRCI) calculations [13]. Finally, the Davidson correction [14], which approximates the contribution of higher excitation terms, was added to get the potential energy functions. All the calculations were done using the 2006.1 version of the MOLPRO code [15].

The energy difference between the two first *ab initio* potentials obtained at large interatomic distances differs from the experimental value by 964 cm^{-1}. As this may affect the calculated cross sections at low energies, a correction was introduced through a diabatization procedure that allowed us to shift the lowest diabatic state by -964 cm^{-1} and to generate new adiabatic states with correct asymptotes after adiabatic back transformation [3]. This procedure takes advantage of the very smooth R variation (R being the internuclear distance) of the electronic couplings in the diabatic representation, and leads to adiabatic potentials that are almost unchanged except at large internuclear distances (see [3] for more details).

There are often difficulties in calculating the quantum-chemical data for the most excited states via these methods, due to the high density of states. Some problems occurred with the calculated potentials for states 6, 7, and 8 (labeling the states from 1–8, lowest to highest) since they have strong mixing and their interactions with upper states prevents their accurate description from 20 a.u. up to dissociation. Despite this, we chose to retain these states, with some physically motivated modifications, since we judge that including them in this manner is preferable to neglecting them totally. To put these modifications on as firm a footing as possible, we have performed some additional quantum-chemical calculations to test several regions of the potentials, with an improved electronic basis set as compared to the basis used in the previous calculations [3]. The basis set for Mg and the active space were extended in order to describe the $3s3d\ ^1D$, $3s4p\ ^3P$, and $3s3d\ ^3D$ asymptotic behavior more correctly, hence concerning the $^2\Sigma^+$ states 6, 7, and 8. The number of states averaged in the reference CASSCF calculations was also extended to get numerical convergence. For the five lowest molecular states these test data practically coincide with the data from [3]. For the states 6, 7, and 8, the new data keep the same general behavior, mostly in the intermediate range region. They are more accurate in the asymptotic region. In particular, the new adiabatic potentials asymptotically agree better with the atomic energies [16], the differences not exceeding 0.024 eV. The modifications made to the quantum-chemical data are therefore as follows. First, since we are interested in the ion-pair production process and there are in fact ten additional atomic states below the ionic limit, we adjusted the long-range behavior of potential 8 to have Coulomb $1/R$ behavior going to this limit, thus allowing population of the ionic channel. This is reasonable since crossings with higher-lying states are expected to be traversed essentially diabatically, and amounts to neglect of these states; this is discussed further below. Potentials for states 6 and 7 were shifted to have correct asymptotic limits corresponding to the Mg $3s3d\ ^1D$ and $3s4p\ ^3P$ atomic states. Finally, the states were modified to have ionic-covalent avoided crossings at the expected internuclear distances. This was achieved through the following procedure. Landau-Zener coupling parameters H_{jk} for the lower crossings amongst states 1–5 were derived from the adiabatic potentials, and an exponential fit to these values with crossing distance R_c was made. From extrapolation via this fit, and knowing the form of the asymptotic covalent diabatic potential (assumed to be constant at the atomic energies) and the ionic diabatic potential ($1/R$ behavior going to the ionic limit), we derived

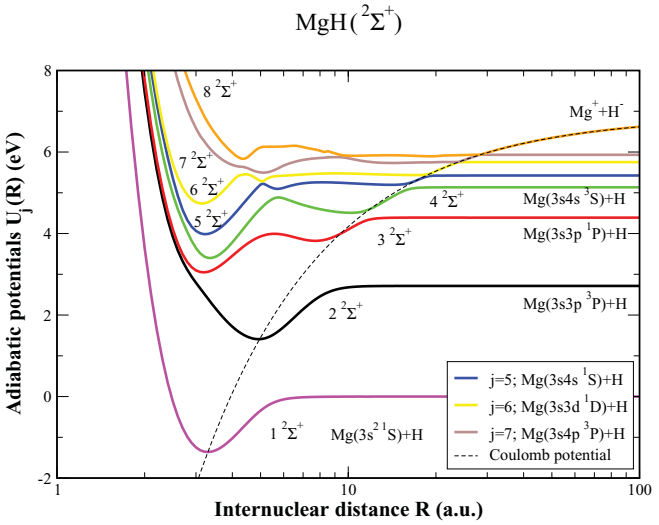

FIG. 1. (Color online) Adiabatic potential energies for the eight MgH($^2\Sigma^+$) states used in the present study. The uppermost (eighth) potential asymptotically corresponds to the ionic $Mg^+ + H^-$ channel. The dashed line shows the Coulomb potential for the $Mg^+ + H^-$ interaction.

adiabatic potentials from the Landau-Zener model. These potentials replace the existing potentials in the expected crossing regions, with smooth functions chosen to join them to the existing *ab initio* potentials at longer and shorter internuclear distances. Thus, these potentials have a similar behavior to their *ab initio* counterpart in the molecular region. At very short internuclear distances ($R < 1.6$ a.u.) the *ab initio* potentials were extrapolated smoothly, taking care to ensure no crossings occur. The corresponding potential energy functions are displayed in Fig. 1. Table I compares the calculated asymptotic energies of the eight lowest $^2\Sigma^+$ states obtained after the diabatization and adjustment procedures with the experimental atomic data.

The nonadiabatic couplings between all the adiabatic states were only calculated at the CASSCF level in order to avoid very time-consuming calculations. However, it was shown [3], by comparing the present CASSCF nonadiabatic couplings with those obtained at the MRCI level for the lowest-lying states, that they display very similar features and

TABLE I. The MgH molecular channels, the corresponding asymptotic atomic states, and the calculated and experimental asymptotic energies with respect to the ground state.

	Molecular	Atomic asymptotic	Asymptotic energies (eV)	
j	states	states	Calculation	Experiment[a]
1	$1\ ^2\Sigma^+$	$Mg(3s^2\ ^1S) + H$	0	0
2	$2\ ^2\Sigma^+$	$Mg(3s3p\ ^3P) + H$	2.7142	2.7142
3	$3\ ^2\Sigma^+$	$Mg(3s3p\ ^1P) + H$	4.3894	4.3458
4	$4\ ^2\Sigma^+$	$Mg(3s4s\ ^3S) + H$	5.1342	5.1078
5	$5\ ^2\Sigma^+$	$Mg(3s4s\ ^1S) + H$	5.4237	5.3937
6	$6\ ^2\Sigma^+$	$Mg(3s3d\ ^1D) + H$	5.7532	5.7532
7	$7\ ^2\Sigma^+$	$Mg(3s4p\ ^3P) + H$	5.9321	5.9321
8	$8\ ^2\Sigma^+$	$Mg^+(3s\ ^2S) + H^-$	6.8916	6.8916

[a]NIST [16] weighted average values.

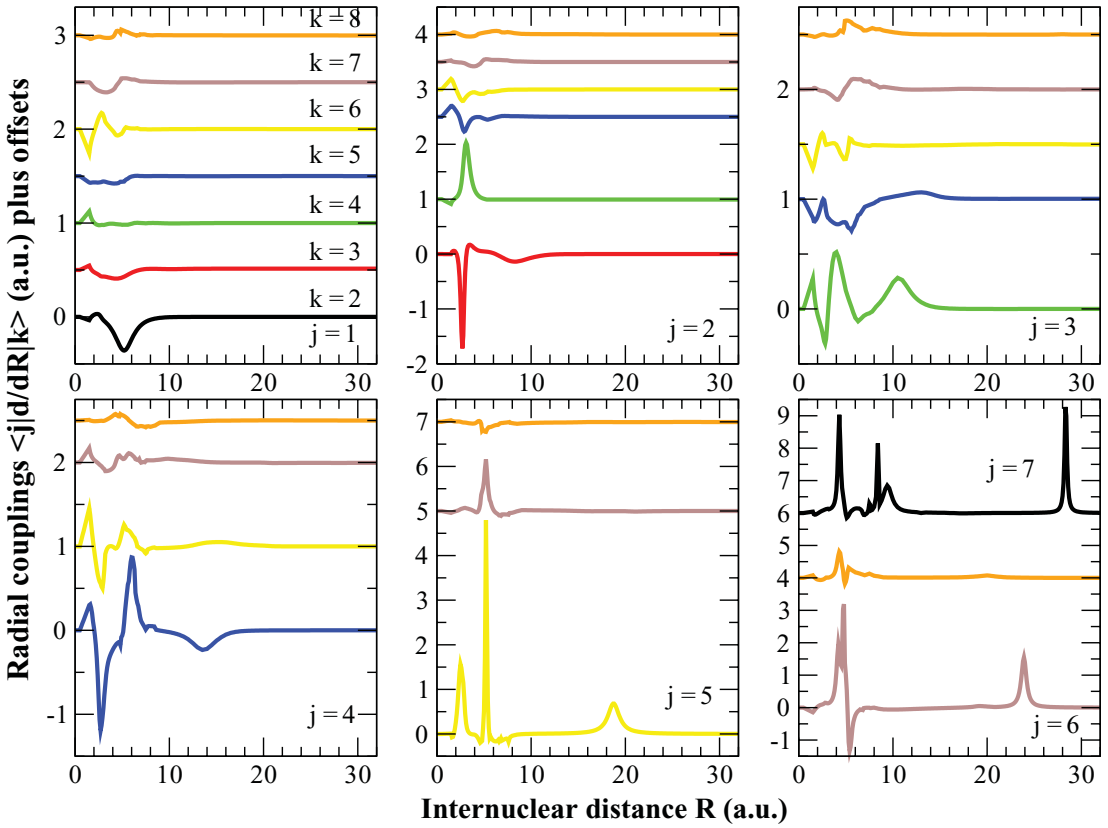

FIG. 2. (Color online) Nonadiabatic radial coupling matrix elements $\langle j|\partial/\partial R|k\rangle$ ($j < k$), plus offsets, between the eight MgH($^2\Sigma^+$) states used in the present study. The molecular state label j is indicated in each panel; note the bottom right panel shows the couplings for both $j = 6$ and $j = 7$. The keys for the labels k are given in the top left panel and are common to all panels, except for the $\langle 7|\partial/\partial R|8\rangle$ coupling, which is shown in black. Offsets are used for better representation of the radial couplings.

the same order of magnitude. Though adjustments were made to the potentials as described above, no adjustments were made to the couplings, apart from the long-range couplings due to interactions between ionic and high-lying covalent configurations. In all calculations, the origin of the electron coordinates was fixed at the center of nuclear mass of the MgH system. The nonadiabatic radial couplings $\langle j|\partial/\partial R|k\rangle$ between the lowest eight molecular states treated in the present work are shown in Fig. 2. The couplings obtained are strong between consecutive states at large internuclear distances, coinciding with the avoided crossings. At short distances, the couplings also have substantial values including couplings between more than two adjacent states together. As explained below, both types of coupling contribute substantially to nonadiabatic nuclear dynamics.

III. NONADIABATIC NUCLEAR DYNAMICS

A. Theoretical approach

The nonadiabatic nuclear dynamics is treated for low-energy Mg + H collisions based on the data for the eight lowest MgH($^2\Sigma^+$) molecular states described above. All inelastic processes for transitions between the seven lowest magnesium atomic states in collisions with the hydrogen atoms, as well as the transitions between these states and the ionic $Mg^+ + H^-$ state are studied for collision energies from the energy thresholds to 10 eV. The following processes are treated: the excitation and the deexcitation processes

$$Mg(3snl\,^{1,3}L) + H \rightarrow Mg(3sn'l'\,^{1,3}L') + H, \qquad (1)$$

the ion-pair production processes

$$Mg(3snl\,^{1,3}L) + H \rightarrow Mg^+ + H^-, \qquad (2)$$

and the mutual neutralization processes

$$Mg^+ + H^- \rightarrow Mg(3snl\,^{1,3}L) + H. \qquad (3)$$

The molecular channels considered and their corresponding asymptotic ($R \rightarrow \infty$) atomic interactions are presented in Table I (see also Fig. 1).

The nonadiabatic nuclear dynamics is studied completely quantum mechanically by means of the multielectron reprojection method [17] (see also [18,19] for the single-electron method) within the standard adiabatic Born-Oppenheimer approach based on the molecular state representation (see, e.g., [20–22]). As is well known, the form of the dynamical equations in this approach is different for different electron coordinate origins [23]. In order to reach the simplest and the standard form of the coupled-channel equations [17–19,23] the electronic structure calculations described above have been carried out with the electron coordinate origin at the center of nuclear mass. In this case, according to the fundamental rules of the standard adiabatic approach, asymptotic values of the

nonadiabatic radial couplings read [17–19,21,23]

$$\langle j|\frac{\partial}{\partial R}|k\rangle_\infty = \gamma_k \frac{m}{\hbar^2}[U_j(\infty) - U_k(\infty)]\langle j|d_z^{at}|k\rangle, \quad (4)$$

$\langle j|d_z^{at}|k\rangle$ being the atomic transition dipole moment, m being the electron-nuclei reduced mass, and $U_j(R)$ being an adiabatic potential for a molecular state j. The scalar factors γ_k depend on to which nucleus an active electron is bound in the asymptotic region; in the present case, they read

$$\gamma_k = -\frac{M_{\rm H}}{M_{\rm Mg} + M_{\rm H}}, \quad (5)$$

$M_{\rm Mg}$ and $M_{\rm H}$ being the masses for Mg and H, respectively. It is seen from Eq. (4) that some nonadiabatic radial coupling matrix elements calculated with the electron origin at the center of nuclear mass have nonzero asymptotic values. As discussed in many papers (see, e.g., [17–19,21,23], and references therein) nonvanishing asymptotic couplings are a fundamental feature of the Born-Oppenheimer approach. Choosing another electron origin does not remove nonzero asymptotic terms coupling different channels in the nuclear dynamical equations due to additional mixed-derivative terms in the total Hamiltonian (see [23]), and so a center of nuclear mass is the most natural choice for the electron origin.

For the eight $^2\Sigma^+$ molecular states treated, there are five nonzero asymptotic nonadiabatic radial couplings between molecular states, which asymptotically correspond to interactions between atomic states with nonzero transition dipole moments (optically allowed transitions). As the magnesium nucleus is much heavier than the hydrogen one, the center of nuclear mass is close to the magnesium nucleus, the scalar factors are small $\gamma_k = -0.0425$, and hence, the asymptotic couplings are rather small. The largest asymptotic coupling is equal to 0.0144 a.u. for the $\langle 1|\partial/\partial R|3\rangle$ matrix element, which couples the $\mathrm{Mg}(3s^2\,{}^1S) + \mathrm{H}$ and the $\mathrm{Mg}(3s3p\,{}^1P) + \mathrm{H}$ states. Nevertheless, even small nonvanishing asymptotic couplings provide nonadiabatic transitions between molecular states at arbitrarily large internuclear separations and at any total angular momentum quantum numbers, and hence, special care regarding nonzero asymptotic couplings must be taken, otherwise calculations of inelastic cross sections do not converge and may even result in unphysical infinite values [17]. The reprojection method takes care of this by projecting correct asymptotic incoming and outgoing wave functions on the molecular-state wave functions in the asymptotic region; nonzero asymptotic nonadiabatic couplings determine the coefficients of such projection. In the present case of Mg + H collisions, the mixing coefficients are rather small. For instance, the largest nonvanishing asymptotic coupling, $\langle 1|\partial/\partial R|3\rangle$, results in the maximum value for the mixing coefficient, which is energy dependent, of 0.0018 (at 10 eV). We have performed calculations of the transition dipole moments between the treated states and higher-lying states (including omitted states) and evaluated corresponding mixing coefficients; they do not exceed 0.0022. Small values of mixing coefficients provide convergence of the calculated cross sections with respect to truncation of the channels included except for the uppermost adiabatic state, which may be coupled with the next higher-lying adiabatic state at short internuclear distances.

In fact, the problem of nonvanishing asymptotic nonadiabatic couplings is part of a more general problem first mentioned in Ref. [24] and later referred to as the electron translation (ET) problem. The point is that a single molecular-state wave function (in particular, calculated from a solution of coupled-channel equations written in the molecular-state representation) does not properly describe a single asymptotic incoming or outgoing wave function. Several remedies have been proposed for solutions of the ET problem within the standard adiabatic approach: (i) the electron translation [24] or common translation [25,26] methods; (ii) the reaction coordinate method [27–29]; and (iii) the reprojection method [17–19]. It should be noted that the hyperspherical approach [30,31] also solves the ET problem, but it is beyond the standard adiabatic approach. This study uses the reprojection method, as it allows one to treat collisions with an arbitrary number of electrons and does not require any additional quantum-chemical calculations; only adiabatic potentials and nonadiabatic couplings with the electron coordinate origin at the center of nuclear mass are needed, which come from quantum-chemical calculations. Within the reprojection method, the coupled-channel equations are solved with nonvanishing asymptotic couplings keeping nonadiabatic transitions between molecular states in the asymptotic region, but the reprojection procedure makes transformations to correct asymptotic wave functions and removes transitions between scattering (atomic) states in the asymptotic regions, finally leading to convergence of the inelastic cross sections.

It should be mentioned that between the highest treated excited state of magnesium interacting with a hydrogen atom, $\mathrm{Mg}(3s4p\,{}^3P) + \mathrm{H}$, and the $\mathrm{Mg}^+(3s\,{}^2S) + \mathrm{H}^-$ ionic channel there are ten more states asymptotically corresponding to excited magnesium atoms interacting with H, from $\mathrm{Mg}(3s3d\,{}^3D) + \mathrm{H}$ to $\mathrm{Mg}(3s5p\,{}^1P) + \mathrm{H}$. These states are not included in the present work for the following reasons. The previous treatment of similar collisions, Li + H [4] and Na + H [7], and their astrophysical applications [5,8] show that the main processes of interest are the excitation between the lowest states and the processes of population to and from the ionic channel. The avoided crossings between the omitted covalent states and the ionic one take place at large internuclear distances, so the system passes these nonadiabatic regions mainly diabatically. This results in rather small cross sections for ion-pair production from the omitted states, as well as for mutual neutralization into these states. Excitation cross sections between highly excited states can be expected to be relatively large (up to a few Å^2), but this should lead to thermodynamical equilibrium distribution of the populations between the states. Thus, the neglect of these states do not significantly affect the inelastic cross sections for the treated states (including the ionic state) except for the highest treated excited state $\mathrm{Mg}(3s4p\,{}^3P)$, for which the calculated cross sections should be considered as the cross sections for population of this state and other higher-lying excited states of magnesium, especially the $\mathrm{Mg}(3s3d\,{}^3D)$ state located close to $\mathrm{Mg}(3s4p\,{}^3P)$.

Thus, the reprojection method used for calculations of nonadiabatic transition probabilities and cross sections, as well as

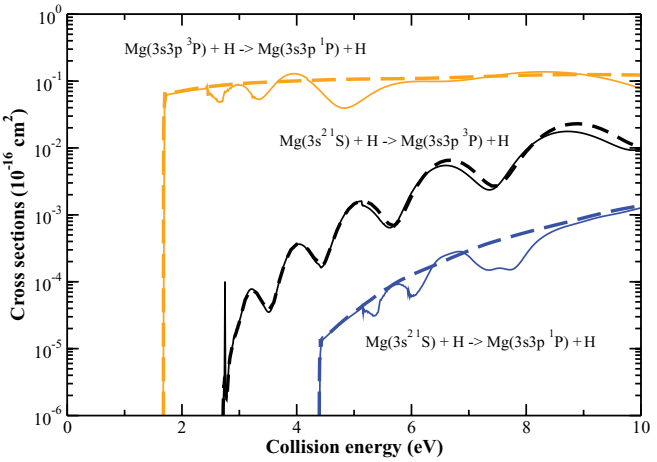

FIG. 3. (Color online) The excitation cross sections between the three lowest Mg atomic states by H impact as a function of the collision energy. The solid lines are the present eight $^2\Sigma^+$ state calculation, while the dashed curves are the five-state (three $^2\Sigma^+$ and two $^2\Pi$) calculation from [3].

small values of the mixing coefficients lead to convergence of the inelastic cross sections with respect to (i) the upper limit for numerical integration of the coupled-channel equations, (ii) the number of partial waves treated for computing the cross sections of astrophysical interest, and (iii) the number of the channels included into consideration (though, as usual, a truncation leads to lower accuracy for inelastic cross sections involving the highest-lying covalent state treated, the state 7 at present).

B. Inelastic cross sections

The calculated partial cross sections $\sigma_{jk}(E)$ $(k > j)$ for the excitation processes (1) between the lowest seven magnesium states, as well as for the ion-pair production processes (2) between these states and the ionic state are presented in Figs. 3 and 4 for collision energies E from the excitation energy thresholds up to 10 eV for each possible entrance channel. The statistical probability factors $p_j^{\rm stat}$ have been included in the calculations. In Fig. 4 the initial state j is shown in each panel; the key is common to all panels and is shown in the top left panel. The bottom right panel of Fig. 4 also shows the cross section for the $7 \to 8$ transition (dashed line) in addition to the cross sections from the state $j = 6$ (solid lines). Only the background cross sections are shown. Orbiting resonances, similar to those found in Na + H collisions [7], have been observed in Mg + H collisions as well; one of these resonances is shown as an example. Deexcitation and mutual neutralization cross sections $\sigma_{kj}(E)$ $(k > j)$ can be inferred using detailed balance

$$\sigma_{kj}(E) = \sigma_{jk}(E + \Delta E_{kj}) \frac{p_k^{\rm stat}}{p_j^{\rm stat}} \frac{E + \Delta E_{kj}}{E}, \qquad (6)$$

where $\Delta E_{kj} = E_k - E_j$ is the energy defect for a process in question, E_j being an atomic energy corresponding to

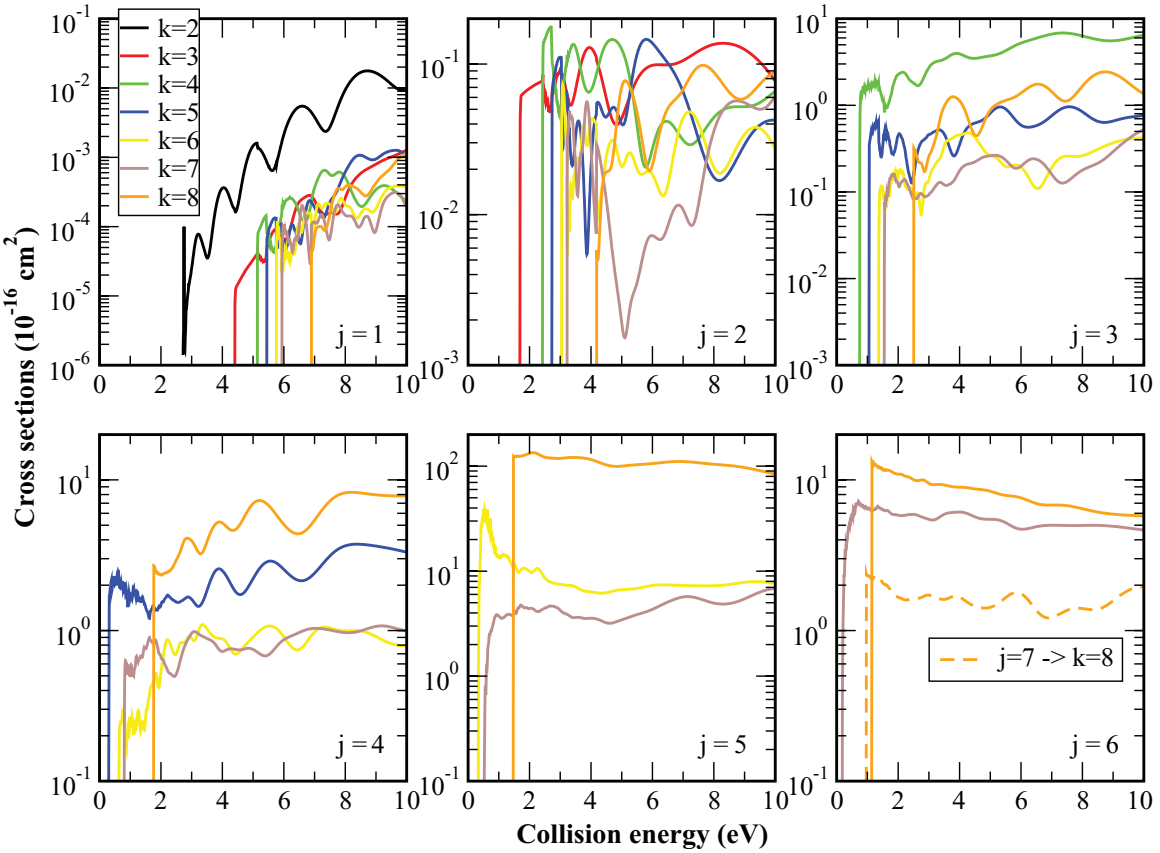

FIG. 4. (Color online) The inelastic cross sections $\sigma_{jk}(E)$ for transitions $j \to k$ $(k > j)$ in low-energy Mg + H collisions. The label j of the initial state from which transitions occur is indicated in each panel. The key for the final states k is given in the top left panel.

a channel j. In the present work, the energy defects are taken as the differences between the asymptotic values of the corresponding adiabatic potentials.

First we compare the cross sections from the present eight-channel calculation with the cross sections from the previous five-state (three $^2\Sigma^+$ and two $^2\Pi$ molecular states) calculation [3], where the excitation processes between the three lowest atomic magnesium states were treated (see Fig. 3). As seen in the figure, the $Mg(3s^2\ ^1S) \rightarrow Mg(3s3p\ ^3P)$ excitation cross section agrees well with the previous one because the process is mainly determined by transitions between the two lowest molecular $^2\Sigma^+$ states taken into account in both calculations. The $Mg(3s^2\ ^1S) \rightarrow Mg(3s3p\ ^1P)$ and $Mg(3s3p\ ^3P) \rightarrow Mg(3s3p\ ^1P)$ excitation cross sections also agree reasonably well with the previous ones apart from the interference oscillations found in the present calculation and not seen in the previous one. These oscillations are due to the presence of the other higher-lying channels that were not treated in the previous calculation [3]. It should be mentioned that the presence of these channels does not reduce the $Mg(3s^2\ ^1S) \rightarrow Mg(3s3p\ ^1P)$ and $Mg(3s3p\ ^3P) \rightarrow Mg(3s3p\ ^1P)$ excitation cross sections, although one could expect that these cross sections (obtained within the three $^2\Sigma^+$ channel treatment) would be redistributed among higher-lying states ($k > 3$), when they are energetically open. This is not a result of inclusion or omission of the molecular $^2\Pi$ states, but a result of different mechanisms for the processes becoming possible as will be discussed below. Thus, the present calculation confirms the conclusion made in Ref. [3] that nonadiabatic transitions between low-lying $^2\Sigma^+$ states dominate over transitions involving other molecular states for the processes of astrophysical interest.

Below is an overview of the features of partial cross sections for the excitation (1) and the ion-pair production (2) processes in low-energy Mg + H collisions (see Fig. 4), as well as the mutual neutralization (3) processes in $Mg^+ + H^-$ collisions. The mechanisms of the processes are discussed in the next section.

(1) The largest cross section with a value of around 100 Å^2 is for the ion-pair production process in $Mg(3s4s\ ^1S) + H$ collisions; that is, for the $5 \rightarrow 8$ process.

(2) The second largest cross sections with order of magnitude of a few Å^2 are for the ion-pair production from $j = 6$, 4, 7, and 3, as well as for the excitation processes from $j = 5$, 6, 3, and 4.

(3) The cross sections from the ground state $Mg(3s^2\ ^1S)$ ($j = 1$) and from the first excited state $Mg(3s3p\ ^3P)$ ($j = 2$) are much smaller than those from higher excited states ($j \geqslant 3$), especially, the cross sections from the ground state, which are typically several orders of magnitude smaller than those from the excited ones. This is mainly the consequence of the fact that the two lowest molecular states are rather well separated energetically from other molecular states (see Fig. 1).

(4) The $Mg(3s^2\ ^1S \rightarrow 3s3p\ ^3P) + H$ cross section is the largest of the excitation cross sections from the ground state and shows Stückelberg oscillations.

(5) For low-lying initial states the ion-pair production processes typically have cross sections of the same magnitude as the excitation cross sections from the same initial state, except from the magnesium ground state. Note that three or four excitation processes from the ground state ($j = 1$) and from the first excited state ($j = 2$) to the final states $k \geqslant 3$ (including the ionic channel) have cross sections of similar order of magnitude. For high-lying initial states, $j \geqslant 4$, the ion-pair production cross sections are larger than the excitation cross sections from the same state.

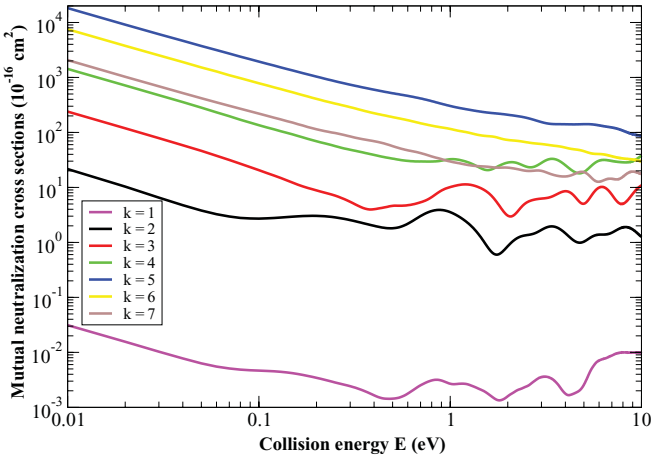

FIG. 5. (Color online) Cross sections $\sigma_{jk}(E)$ ($j = 8$) for the mutual neutralization processes in $Mg^+ + H^-$ collisions as a function of the collision energy.

(6) It is worth noticing that the cross sections for the processes with transitions between atomic states of different spin symmetries (singlets and triplets) have values of the same order of magnitude as cross sections for transitions between states of the same spin symmetry. This is quite natural for atomic collisions, which are described in terms of molecular states created by atoms of the same or different spin symmetries. Both singlet and triplet atomic states of magnesium interacting with hydrogen atoms create molecular $MgH(^2\Sigma^+)$ states with nonadiabatic transitions between them. The situation is different from electron-atom collisional processes, where interspin transition cross sections are usually smaller than cross sections within the same spin symmetry.

(7) Mutual neutralization cross sections are important for astrophysical applications. For this reason Fig. 5 shows the cross sections $\sigma_{jk}(E)$ ($j = 8$) for the mutual neutralization processes (3). It is seen from this figure that the largest cross section in $Mg^+ + H^-$ collisions is for the neutralization into the $Mg(3s4s\ ^1S) + H$ state, $k = 5$. The second largest cross sections are for the neutralization into the $Mg(3s3d\ ^1D)$ state [roughly, three times less than cross section for neutralization into $Mg(3s4s\ ^1S)$], into $Mg(3s4s\ ^3S)$ and into $Mg(3s4p\ ^3P)$.

(8) The present calculation treats the molecular state 7 as the highest-lying asymptotic covalent state, although there are some other covalent states between $Mg(3s4p\ ^3P) + H$ and the asymptotic limit for the ionic state $Mg^+ + H^-$. In this case the inelastic cross sections calculated with transitions into the $Mg(3s4p\ ^3P)$ state ($j = 7$) should be understood as the inelastic cross sections with transitions into this state and into other higher-lying states below the ionic limit; that is, up to $Mg(3s5p\ ^1P)$. It is expected that these cross sections will

be substantially distributed between several states, in particular, between Mg($3s4p\,^3P$), Mg($3s3d\,^3D$), and Mg($3s4p\,^1P$), which are energetically close. In addition to this redistribution, the cross sections into and from the Mg($3s4p\,^3P$) state have lower accuracy due to both the truncation of the channels and the more approximate description of the high-lying ionic-covalent avoided crossings, though the new mechanisms found in the present paper and described below reduce sensitivity of these cross sections to a description of the high-lying ionic-covalent avoided crossings. On the other hand, omission of these higher-lying states should not affect the calculated inelastic cross sections between other states included in the present treatment.

C. Process mechanisms

There are several mechanisms found for the processes (1)–(3) in low-energy Mg + H collisions. It should be emphasized that all these mechanisms are due to nonadiabatic transitions between the MgH($^2\Sigma^+$) molecular states and, hence, based on radial nonadiabatic couplings. Transitions induced by rotational couplings were discussed in Ref. [3], where the dominant role of the transitions between low-lying MgH($^2\Sigma^+$) molecular states was shown. Nevertheless, even for transitions between MgH($^2\Sigma^+$) molecular states it is possible to distinguish different mechanisms that determine the calculated partial inelastic cross sections. In order to recognize the underlying mechanisms for different processes, in addition to the calculation described above where all nonadiabatic radial couplings are included, several test dynamical calculations have been performed. In particular, the following calculations were made: (i) calculation with only couplings between adjacent states; (ii) calculation with only long-range couplings (due to the ionic-covalent configuration interaction) between adjacent states; (iii) calculation with only short-range couplings (excluding ones of the ionic-covalent configuration interaction) between adjacent states; (iv) calculation with only long-range couplings; and (v) calculation with only short-range couplings. Analysis of the test calculations permits us to distinguish various mechanisms for the inelastic processes in Mg + H and $Mg^+ + H^-$ collisions.

The MgH($^2\Sigma^+$) adiabatic potentials (see Fig. 1), clearly show a series of avoided crossings due to interactions between covalent and ionic $Mg^+ + H^-$ configuration, similar to alkali hydrides, e.g., LiH [4,33] and NaH [6,7,34]. The Coulomb potential for the $Mg^+ + H^-$ interaction drawn by the dashed line in Fig. 1 indicates the origin of these avoided crossings. Nonadiabatic radial couplings depicted in Fig. 2 prove that these avoided crossings are indeed nonadiabatic regions. The potential energy splittings at the centers of these nonadiabatic regions, which mainly determine nonadiabatic transitions in these regions, for example, within the Landau-Zener model, dramatically increase with decreasing internuclear distance, as is expected from the general (asymptotic) theory (see, e.g., [32]). This results in large potential energy splittings at short distances and in small splittings otherwise. Finally, this leads to the fact that the system traverses nonadiabatic regions mainly adiabatically at short range, and practically diabatically at long range. At some intermediate distances (around $R \approx 10-20$ a.u.) adiabatic energy splittings are optimal for nonadiabatic transitions. In addition to the nonadiabatic regions corresponding to the ionic configuration, there are nonadiabatic regions between molecular states at short range, where not only adjacent states are coupled (see Figs. 1 and 2). These regions also affect nonadiabatic dynamics. It is worth emphasizing that typically several mechanisms compete with each other, making different mechanisms dominant for different collision conditions: collision energies E and total angular momentum quantum numbers J. Finally, the following reaction mechanisms are found.

The first mechanism. Nonadiabatic transitions occur between two adjacent adiabatic molecular states in a single nonadiabatic region due to the ionic-covalent configuration interaction. An example of this mechanism is the Mg($3s^2\,^1S \rightarrow 3s3p\,^3P$) + H excitation process, which is predominantly determined by a single broad nonadiabatic region between the first and the second molecular states around $R \approx 5.4$ a.u., though there are other nonadiabatic regions between these two states, as well as between these and other states. The test calculations show that taking into account only long-range couplings between adjacent states does not substantially change this inelastic cross section as compared with the all-coupling calculation, although at small J the nonadiabatic transition probabilities become slightly different with this procedure. This mechanism explains the Stückelberg oscillations for the $\sigma_{12}(E)$ cross section seen in Fig. 4.

The second mechanism is also determined by nonadiabatic regions due to the ionic-covalent interaction, but related to both a single nonadiabatic region with optimal potential splitting, where the probability current is branched in the optimal way, and several high-lying nonadiabatic regions, which are passed by the system practically diabatically resulting in the ionic state. An example of this mechanism is the ion-pair production process Mg($3s4s\,^1S$) + H $\rightarrow$ $Mg^+ + H^-$ with the largest cross section $\sigma_{58}(E)$. After a double traversal of the nonadiabatic region around $R \approx 18.8$ a.u. the current from the fifth state substantially populates the sixth adiabatic molecular states and this outgoing current passes the higher-lying nonadiabatic regions practically diabatically, finally providing large transition probabilities for populating the ionic state. Again the test calculation with only the long-range adjacent couplings proves this mechanism, especially at rather large J, which mainly determine the inelastic cross section.

The third mechanism is also related to the ionic-covalent interaction and leads to excitation via the intermediate ionic-configuration-based molecular state. Typical examples are the transitions $5 \rightarrow 6$ and $4 \rightarrow 5,6$. Although these cross sections are smaller than the cross section for the ion-pair production from the same states, roughly by an order of magnitude, nevertheless, they have rather large values of an order of a few Å^2 (see Fig. 4). The calculation with long-range couplings between adjacent states supports this idea providing close, though not identical values for the inelastic cross sections as from the all-coupling calculation.

The fourth mechanism. Although the previous mechanism provides excitation between all excited atomic states below the ionic limit, another mechanism dominates for relatively high excited states. The high-lying ionic-covalent avoided crossings are passed diabatically leading to small nonadiabatic transition

probabilities for the excitation processes. On the other hand, these covalent-configuration-based states are coupled at short range, and these nonadiabatic regions yield larger transition probabilities, though at relatively limited ranges of J. Finally, this distribution of currents between covalent states at short distances, provides the main contributions to excitation cross sections. Typically these short-range nonadiabatic couplings take place at a few a.u., so the corresponding inelastic cross sections do not exceed a few Å^2. An example is the $Mg(3s3d\,^1D \rightarrow 3s4p\,^3P) + H$ excitation ($6 \rightarrow 7$). The nonadiabatic regions around $R \approx 24$ and 28 a.u. are passed diabatically and the nonadiabatic transitions between corresponding covalent states occur at the internuclear distances $R < 10$ a.u. providing a cross section of a few Å^2 (see Fig. 4).

The fifth mechanism. The short-range couplings are also important for the ion-pair production from high excited states: the fifth mechanism is a combination of short-range couplings between covalent states and a series of ionic-covalent avoided crossings at long range. An example is the $7 \rightarrow 8$ process: the incoming current passes the nonadiabatic region around $R \approx 28$ a.u. diabatically, then at short distances it goes down to the fourth and the fifth adiabatic states, and the outgoing current traverses diabatically a series of nonadiabatic regions at long range, thus populating the ionic state. The probability current makes a kind of a loop.

The sixth mechanism. This mechanism is related to short-range nonadiabatic couplings between low-lying adiabatic states, which are energetically well separated with rather small transition probabilities. In this case, nonadiabatic transitions around the classical turning points become comparable to the transition probabilities due to the ionic-covalent interaction. The former are determined by both two-step transitions between adjacent states and one-step transitions due to nonadiabatic couplings between nonadjacent states. Figure 2 shows that the short-range nonadiabatic couplings (and not only between neighboring states) have substantial values. An example is the $1 \rightarrow 3$ excitation process. To a large degree, this process is determined by the two-step, $1 \rightarrow 2$ and $2 \rightarrow 3$, transitions, as well as the one-step $1 \rightarrow 3$ transitions around the classical turning points. This explains why the $1 \rightarrow 3$ inelastic cross section does not exhibit Stückelberg oscillations, while the $1 \rightarrow 2$ inelastic cross section does. This mechanism also explains why the three-$^2\Sigma^+$-channel calculation [3] and in the present eight-$^2\Sigma^+$-channel treatment give close results for the cross sections of the $Mg(3s^2\,^1S) \rightarrow Mg(3s3p\,^3P)$ excitation process: transitions due to short-range couplings are found to dominate (mechanism 6) rather than long-range couplings (mechanism 3).

Thus, the long-range nonadiabatic regions due to interactions of the ionic and covalent configurations determine to a large extent the reaction mechanisms, in particular, providing the inelastic cross sections with the largest magnitudes. On the other hand, some state-to-state processes are determined either by the mechanisms due to the short-range nonadiabatic couplings between covalent states or by the mechanisms based on combinations of the short-range and the long-range nonadiabatic couplings.

The mechanisms for the inverse (exothermic) processes are the same as for the direct (endothermic) processes. In particular, this analysis of the mechanisms explains the variation of the mutual neutralization cross sections. The incoming probability current from the ionic state passes high-lying (long-range) ionic-covalent avoided crossings [including those created by covalent states higher than $Mg(3s4p\,^3P) + H$ and omitted here] diabatically down to the internuclear distances around $R \approx 10$–20 a.u., where the adiabatic potential splittings become optimal. At these distances, the probability current is distributed between several adiabatic states populating mainly several final states due to either the direct mechanism 2 or the loop mechanism 5. Finally, the largest mutual neutralization cross section corresponds to population of the $Mg(3s4s\,^1S) + H$ state with the optimal nonadiabatic parameters, and the second largest cross sections are associated with population of the energetically neighboring states: $Mg(3s3d\,^1D) + H$, $Mg(3s4s\,^3S) + H$, and $Mg(3s4p\,^3P) + H$ (see Fig. 5). Population of the ground state is weak due to large potential energy splittings.

IV. CONCLUSIONS

We have performed a full quantum treatment of inelastic process in low-energy $Mg + H$ and $Mg^+ + H^-$ collisions. The treatment is based on *ab initio* quantum-chemical calculations of the eight lowest $MgH(^2\Sigma^+)$ adiabatic potentials and the nonadiabatic radial couplings between all corresponding states. We adjusted the three upper potentials in such a way that the uppermost potential has long-range Coulomb behavior corresponding to the ionic $Mg^+ + H^-$ interaction, and that two others have correct asymptotic limits to the $3s3d\,^1D$ and $3s4p\,^3P$ atomic states of magnesium; finally, the states were modified to have ionic-covalent avoided crossings at proper internuclear distances. The adjustment allowed us to treat the ionic channel, as well as to obtain correct energy thresholds for the high-lying states. These quantum-chemical data allowed us to accomplish full quantum scattering calculations of low-energy inelastic cross sections for the excitation, the ion-pair production, and the mutual neutralization processes in the title collisions by means of the reprojection method which takes into account the nonzero asymptotic radial couplings and the correct asymptotic total wave functions. An extensive set of cross sections between the seven lowest levels and the ionic channel up to collision energies of 10 eV were calculated. The reprojection method provides convergence for the calculated inelastic cross sections with respect to both the upper integration limit for solutions of the coupled-channel equations and the number of partial waves treated, while small values of the mixing coefficients lead to convergence with respect to truncation of the molecular channels considered. The present truncation can affect cross sections into and from the $Mg(3s4p\,^3P)$ state.

The cross sections for the excitation and the ion-pair production processes show a large variation in amplitude for different transitions, from as large as 120 to as small as 10^{-6} Å^2. We point out that cross sections for transitions between spin-allowed and spin-forbidden atomic states are of the same order of magnitude owing to relevant molecular mechanisms. The largest cross section for the endothermic processes in $Mg + H$ collisions is for the ion-pair production

process from the $Mg(3s4s\ ^1S)$ state. The largest value of the inelastic cross sections in $Mg^+ + H^-$ collisions corresponds to mutual neutralization into the $Mg(3s4s\ ^1S) + H$ state. Mutual neutralization processes into a few other states also have relatively large cross sections.

Physical mechanisms for the inelastic processes in the treated collisions were carefully studied and several mechanisms were found. It is shown that some of the mechanisms are determined, as usually expected, by transitions between adjacent molecular states at long-range distances due to interactions between ionic and covalent configurations. However, thanks to the availability of *ab initio* calculated radial couplings at all internuclear distances, mechanisms due to transitions at short distances involving several molecular states, not restricted to adjacent states, are found to be important. Those additional mechanisms explain the relatively large cross sections for excitation of high atomic states. The cross sections calculated in the present work are expected to be of sufficient precision to evaluate their astrophysical importance; such application is already under way.

ACKNOWLEDGMENTS

This research was supported by the CNRS national program "Programme National de Physique Stellaire," the Royal Swedish Academy of Sciences, Göran Gustafssons Stiftelse, and the Swedish Research Council. A.K.B. also gratefully acknowledges the support from the Russian Foundation for Basic Research (Grant No. 10-03-00807-a), from the Wenner-Gren Foundation (Sweden), and from the MSME laboratory (Université Paris-Est and UMR 8208 of the CNRS). P.S.B. is supported by a grant from the Knut and Alice Wallenberg Foundation. The *ab initio* quantum-chemistry calculations were performed at the IDRIS-CNRS French national computing center (Institut de Développement et des Ressources en Informatique Scientifique du Centre National de la Recherche Scientifique) under project 040883 and on work stations at MSME laboratory (University of Paris-Est Marne la Vallée) and at Centre Informatique of Paris Observatory. The authors acknowledge the role of the SAM collaboration (http://www.anst.uu.se/ulhei450/GaiaSAM/) in stimulating this research through regular workshops.

[1] M. Asplund, Annu. Rev. Astron. Astrophys. **43**, 481 (2005).
[2] E. Arnone, S. G. Ryan, D. Argast, J. E. Norris, and T. C. Beers, Astron. Astrophys. **430**, 507 (2005).
[3] M. Guitou, A. K. Belyaev, P. S. Barklem, A. Spielfiedel, and N. Feautrier, J. Phys. B **44**, 035202 (2011).
[4] A. K. Belyaev and P. S. Barklem, Phys. Rev. A **68**, 062703 (2003).
[5] P. S. Barklem, A. K. Belyaev, and M. Asplund, Astron. Astrophys. **409**, L1 (2003).
[6] A. K. Belyaev, J. Grosser, J. Hahne, and T. Menzel, Phys. Rev. A **60**, 2151 (1999).
[7] A. K. Belyaev, P. S. Barklem, A. S. Dickinson, and F. X. Gadéa, Phys. Rev. A **81**, 032706 (2010).
[8] P. S. Barklem, A. K. Belyaev, A. S. Dickinson, and F. X. Gadéa, Astron. Astrophys. **519**, A20 (2010).
[9] M. Guitou, A. Spielfiedel, and N. Feautrier, Chem. Phys. Lett. **488**, 145 (2010).
[10] D. E. Woon and T. H. Dunning Jr., from Basis Set Exchange: A Community Database for Computational Sciences, K. L. Schuchardt, B. T. Didier, T. Elsethagen, L. Sun, V. Gurumoorthi, J. Chase, J. Li, and T. L. J. Windus, Chem. Inf. Model. **47**, 1045 (2007).
[11] T. H. Dunning Jr., J. Chem. Phys. **90**, 1007 (1989).
[12] H.-J. Werner and P. J. Knowles, J. Chem. Phys. **82**, 5053 (1985); P. J. Knowles and H.-J. Werner, Chem. Phys. Lett. **115**, 259 (1985).
[13] H.-J. Werner and P. J. Knowles, J. Chem. Phys. **89**, 5803 (1988); P. J. Knowles and H.-J. Werner, Chem. Phys. Lett. **145**, 514 (1988).
[14] S. R. Langhoff and E. R. Davidson, Int. J. Quantum Chem. **8**, 61 (1974); M. R. A. Blomberg and P. E. M. Siegbahn, J. Chem. Phys. **78**, 5682 (1983).
[15] MOLPRO is a package of *ab initio* programs written by H.-J. Werner and P. J. Knowles, with contributions from J. Almlöf, R. D. Amos, M. J. Deegan, S. T. Elbert, C. Hampel, W. Meyer, K. Peterson, R. Pitzer, A. J. Stone, P. R. Taylor, R. Lindh, M. E. Mura, and T. Thorsteisson [http://www.molpro.net].
[16] Y. Ralchenko, A. E. Kramida, and J. Reader (NIST ASD Team), NIST Atomic Spectra Database (version 3.1.4), Gaithersburg, MD, USA: National Institute of Standards and Technology, 2008 [http://physics.nist.gov/asd3].
[17] A. K. Belyaev, Phys. Rev. A **82**, 060701(R) (2010).
[18] J. Grosser, T. Menzel, and A. K. Belyaev, Phys. Rev. A **59**, 1309 (1999).
[19] A. K. Belyaev, D. Egorova, J. Grosser, and T. Menzel, Phys. Rev. A **64**, 052701 (2001).
[20] N. F. Mott and H. S. W. Massey, *The Theory of Atomic Collisions* (Clarendon, Oxford, 1949).
[21] A. Macías and A. Riera, Phys. Rep. **90**, 299 (1982).
[22] B. H. Bransden and M. R. C. McDowell, *Charge Exchange and the Theory of Ion-Atom Collisions* (Clarendon, Oxford, 1992).
[23] A. K. Belyaev, A. Dalgarno, and R. McCarroll, J. Chem. Phys. **116**, 5395 (2002).
[24] D. R. Bates and R. McCarroll, Proc. R. Soc. London, Ser. A **245**, 175 (1958).
[25] S. B. Schneiderman and A. Russek, Phys. Rev. **181**, 311 (1969).
[26] L. F. Errea, L. Mendez, and A. Riera, J. Phys. B **15**, 101 (1982).
[27] M. H. Mittleman, Phys. Rev. **188**, 221 (1969).
[28] W. R. Thorson and J. B. Delos, Phys. Rev. **18**, 135 (1978); J. B. Delos, Rev. Mod. Phys. **53**, 287 (1981).
[29] M. Gargaud, R. McCarroll, and P. Valiron, J. Phys. B **20**, 1555 (1987); D. Rabli and R. McCarroll, *ibid.* **38**, 3311 (2005); P. Barragán, L. F. Errea, F. Guzman, L. Mendez, I. Rabadan, and I. Ben-Itzhak, Phys. Rev. A **81**, 062712 (2010).
[30] J. Macek, M. Cavagnero, K. Jerjian, and U. Fano, Phys. Rev. A **35**, 3940 (1987).
[31] C. D. Lin, Phys. Rep. **257**, 1 (1995).
[32] C. Herring, Rev. Mod. Phys. **34**, 631 (1962); M. I. Chibisov and R. K. Janev, Phys. Rep. **166**, 1 (1988).
[33] H. Croft, A. S. Dickinson, and F. X. Gadéa, J. Phys. B **32**, 81 (1999).
[34] A. S. Dickinson, R. Poteau, and F. X. Gadéa, J. Phys. B **32**, 5451 (1999).